SI Appendix

Text S1 Glutamate restores susceptibility of drug-resistant *E. tarda* to kanamycin.

Text S2 Mass isotopomer analysis for ^{13}C labeled glutamate detected in a nontargeted manner.

Text S3 Pharmacologic inhibition of enzyme catalysis is a widely accepted.

SI Materials and methods

Fig. S1 Glutamate restores susceptibility of drug-resistant *E. tarda* to kanamycin**.**

Fig. S2 Glutamate restores susceptibility to kanamycin and regulates NADH, PMF and cellular kanamycin.

Fig. S3 Lactate measurement.

Fig. S4 Effect of inhibitors on the P cycle.

Fig. S5 Mass isotopomer analysis for ^{13}C labeled glutamate detected in a nontargeted manner in *E. coli* K12 cultured in different culture conditions.

Fig. S6 Percent survival of rescued strains and oleate-enabled killing of *E. coli* K12 by gentamicin.

Table S1. Summary of all compounds being detected as labeled by the [U-^{13}C] labeled L-glutamate in *E. tarda* EIB202, which were cultured in LB medium and then incubated in M9 plus acetate with the labeled glutamate

Table S2. Non-targeted detection of [U-^{13}C] labeled L-glutamate in *E. tarda* EIB202,

which were cultured in LB medium and then incubated in M9 plus acetate with the labeled glutamate

Table S3. Non-targeted detection of [U-^{13}C] labeled L-glutamate in *E. coli* K12 BW25113, which were cultured in LB medium and then in M9 medium plus acetate with the labeled glutamate.

Table S4. Non-targeted detection of [U-^{13}C] labeled L-glutamate in *E. coli* K12 BW25113, which were cultured in M9 medium with acetate plus 0.3% glucose and then incubated in M9 medium plus acetate with the labeled glutamate.

Table S5. Non-targeted detection of [U-^{13}C] labeled L-glutamate in *E. coli* K12 BW25113, which were cultured in SOC medium and then incubated in M9 medium plus acetate with the labeled glutamate.

Table S6. Non-targeted detection of [U-^{13}C] labeled L-glutamate at 2 h in *E. coli* K12 BW25113, which were cultured in LB medium and then incubated in M9 medium plus acetate with the labeled glutamate

Table S7. Non-targeted detection of [U-^{13}C] labeled L-glutamate at 4h in *E. coli* K12 BW25113, which were cultured in LB medium and then incubated in M9 medium plus acetate with the labeled glutamate.

Table S8. Non-targeted detection of [U-^{13}C] labeled L-glucose in *E. coli* K12 BW25113, which were cultured in LB medium and then incubated in M9 medium plus acetate with the labeled glucose.

Table S9. Primers used for qPCR.

Table S10. Primers used for gene complementation.

Text S1, Glutamate restores susceptibility of drug-resistant *E. tarda* to kanamycin.

In our previous study, we showed depressed glutamate as alanine and glucose did in *E. tarda* LTB4-R (lab-generated kanamycin-resistant strain) and EIB202 (isolated multidrug-resistant strain from dead fish) (**SI Appendix Fig. S1A**) (1). Alanine and glutamate are in the same pathway alanine, aspartate and glutamate metabolism, which are reversibly converted to pyruvic acid and α-ketoglutarate, respectively, by glutamic-pyruvic transaminase (GPT) and feed the TCA cycle (**SI Appendix Fig. S1B**). To investigate the adjunct effect of glutamate on kanamycin, viability of *E. tarda* LTB4-R and EIB202 was assessed in the presence of different incubation periods, kanamycin concentrations and glutamate concentrations. The viability of LTB4-R and EIB202 decreased over time (**SI Appendix Fig. S1C**), and in a kanamycin dose-dependent manner (**SI Appendix Fig. S1D**). An approximate 2,000-fold decrease in viability was observed for LTB4-R and EIB202 in the presence of 1,000 and 50 μg/mL kanamycin, respectively (**SI Appendix Fig. S1D**). The viability of LTB4-R and EIB202 was decreased with increasing glutamate, when approximate 120-fold and 600-fold decreased were detected in viability under the synergistic effect of 2.5 glutamate and 500 μg/mL and 30 μg/mL kanamycin for 6 h, respectively, but was unaffected if glutamate or kanamycin was present individually (**SI Appendix Fig. S1E**).

Reprogramming the energy flow in antibiotic-resistant bacteria is an important mechanism by which alanine could increase the antibiotic uptake through increased

PMF (1). However, in this aspect a similar mechanism for glutamate is still relatively explored. Concentration of NADH and PMF was quantified in EIB202 in the presence or absence of glutamate. In addition, PMF was detected in the presence or absence of carbonyl cyanide m-chlorophenyl hydrazone (CCCP), an inhibitor of PMF. Results showed that glutamate promoted NADH production and PMF generation (**SI Appendix Figs. S1F** and **S1G)**, and CCCP blocked PMF generation (**SI Appendix S1G**). Glutamate promoted kanamycin uptake, but abrogated by CCCP (**SI Appendix Fig. S1H**). Consistently, cell viability was reduced under the synergistic effect of glutamate plus kanamycin, which was inhibited by CCCP (**SI Appendix S1I**).

Western blot analysis showed that glutamate stimulates expression of NuoI and NuoF and promotes activity of respiratory chain dehydrogenase in a dose-dependent manner (**SI Appendix Fig. S2A**), which was consistent with PMF measurements and enzyme activity under comparable conditions (**SI Appendix Figs. S2B** and **S2C**). When respiration was blocked with rotenone, antimycin A or NaN_3, the effect of glutamate plus kanamycin on PMF and cell viability was abrogated (**SI Appendix Figs. S2D** and **S2E**). The effect of glutamate plus kanamycin on cell viability is pH-dependent (**SI Appendix Fig. S2F**). The PMF promoted by glutamate is not observed under anaerobic conditions (**SI Appendix Fig. S2G**). Malonate, a competitive inhibitor of the enzyme succinate dehydrogenase, downregulated NADH and PMF (**SI Appendix Fig. S2H)**, abrogating the effect of glutamate on viability of EIB202 (**SI Appendix Fig. S2I**), and concurrent intracellular drug concentrations decreased, while cell

viability increased, consistent with these results (**SI Appendix Fig. S2J**). OD value of antibiotic-sensitive LTB4-S and antibiotic-resistant LTB4-R was higher in M9 medium with or without acetate and glucose, and then glutamate with or without acetate than in M9 medium with or without acetate (**SI Appendix Fig. S2K**). However, these different culture conditions didn't impact their minimum inhibitory concentration (MIC). When kanamycin is added to nongrowing cells, glutamate or glucose or plus acetate elevated kanamycin-induced killing of EIB202 by approximately 2 folds, compared with or without acetate (**SI Appendix Fig. S2L**). Glutamate could potentiate other antibiotics including gentamicin, ampicillin, rifampicin and erythromycin to kill EIB202 (**SI Appendix Fig. S2M**). Among them, gentamicin and erythromycin targets are protein synthesis (the two drugs belong to aminoglycosides and macrolides, and target at 30S rRNA and 50S rRNA, respectively), while ampicillin and rifampicin targets are the cell wall and the RNA polymerase, respectively. These results indicate that glutamate has the potential in promoting different antibiotics with differential work mechanisms.

Thus, glutamate increased intracellular NADH concentration and PMF, promoted kanamycin uptake, which likely contribute to the killing of kanamycin-resistant bacteria. Compared to our previously reported efficacy of alanine (1), glutamate generated somewhat higher NADH and PMF compared to alanine (**SI Appendix Figs. S2N**). Correspondingly, the viability of EIB202 was lower in the presence of glutamate than in the presence of alanine or aspartate, another depressed metabolite in

alanine, aspartate and glutamate metabolism, and was no significant difference with glucose plus kanamycin (**SI Appendix Fig. S2O**). These results suggest the effect of metabolic difference on the action between glutamate and alanine.

Text S2. Mass isotopomer analysis for ^{13}C labeled glutamate detected in a nontargeted manner.

Three potential cycles/pathways were identified. In the first cycle, $^{13}C_5$-glutamate entered the TCA cycle via α-ketoglutarate to produce M4-labeled succinate, fumarate, and malate, oxaloacetate, and then citrate. The low abundance of M4-labeled citrate indicated the transformation of M4-labeled oxaloacetate with unlabeled acetyl-CoA (AcCoA) to citrate was limited by the TCA cycle. The data indicate a high ^{13}C-response from M4-oxaloacetate in alanine, glycine, threonine, pyruvate and fatty acids. It is possible that ^{13}C-alanine, -glycine and -threonine may be transferred to phosphoenolpyruvate (PEP) and then pyruvate, but ^{13}C-pyruvate and -fatty acids are not irreversibly converted to PEP (http://www.genome.jp/kegg). Thus, the labeled alanine, glycine and threonine should be coming from ^{13}C-oxaloacetate through ^{13}C-PEP rather than ^{13}C-pyruvate. We further deduced that M2-labeled AcCoA was generated from M3-labeled pyruvate, which was converted from M3-labeled PEP and subsequently processed to M2-labeled citrate, with unlabeled oxaloacetate present downstream from the TCA cycle due to limited flux through the TCA cycle, which is supported by a relatively low amount of M6-labeled citrate. It should be noted that if M4-labeled oxaloacetate was utilized in the transformation, significantly more M6-labeled citrate would be expected. In the second cycle, M2-labeled oxaloacetate

from M2-labeled citrate generated M2-labeled pyruvate and M1-labeled AcCoA, by oxidative decarboxylation of pyruvate to AcCoA, with subsequent generation of M1-labeled citrate. In the third cycle, M1-labeled oxaloacetate from M1-labeled citrate generated M1-labeled pyruvate, as well as unlabeled AcCoA and citrate, since the pathway also involved oxidative decarboxylation of pyruvate to AcCoA. The M3 label may have also been generated from M2-labeled oxaloacetate and M1-labeled AcCoA or M1-labeled oxaloacetate and M2-labeled AcCoA via the TCA cycle. However, less M3 label was detected than M1 or M2 label due to limited flux through the TCA cycle. Meanwhile, M2-labeled glycine from M4 labeled oxaloacetate was transformed to M2-labeled serine and then M2-labeled pyruvate, contributing to the higher abundance of M2-labeled pyruvate. The M2-labeled pyruvate generated M1-labeled AcCoA through oxidative decarboxylation, generating more M1 label than M2 label. Equal amounts of M4, M2, and M1/M2 were required to generate M2, M1, and M3 compounds, respectively. As shown in **Fig. 1B**, the ratio of each pool (i.e. M1 + M2 + M3) / (M1 + M2 + M4 + M2 from glycine) represents relative flux for that metabolite in the TCA cycle plus the OAA-PEP-Pyr-AcCoA-citrate pathway ($\upsilon_{TCA\text{-}PLUS}/\upsilon_{GLUTAMATE}$), where $\upsilon_{TCA\text{-}PLUS}$ refers to the turnover of a particular metabolite pool and $\upsilon_{GLUTAMATE}$ refer to the flux of glutamate carbon atoms to the cycle (**Fig. 1B**).

Text S3 Pharmacologic inhibition of enzyme catalysis is a widely accepted.

Pharmacologic inhibition of enzyme catalysis is a widely accepted approach (2), and

155 the inhibitors used in the present study are well characterized (1, 3-7). In microbes,
156 malonate showed high specificity for succinate dehydrogenase (3, 5) and
157 Bromopyruvate and furfural are more specific than Na_2-ATP in target proteins.
158 Bromopyruvate acts initially as a competitive inhibitor with pyruvate (*Ki* = 90 μM)
159 but then proceeds to react irreversibly with the enzyme. Bromopyruvate also inhibits
160 dihydrodipicolinate synthase (DHDPS), which catalyzes the condensation of pyruvate
161 and aspartate beta-semialdehyde, with a *Ki* of 1600 μM, indicating 18-fold inhibitory
162 decreases in PDH efficacy (4). Furfural is an inhibitor of PDH, alcohol dehydrogenase
163 (ADH), and aldehyde dehydrogenase (AIDH), although there is no AIDH in *E. tarda*
164 EIB202. Furfural decreases the activity of PDH by more than 90%, whereas ADH
165 activity decreased by less than 20% at the same concentration. Furfural inhibits ADH
166 competitively and PDH non-competitively (7), while Na_2-ATP is an inhibitor of PCK,
167 citrate synthase, isocitrate dehydrogenase, and α-oxoglutarate dehydrogenase. These
168 data indicate that bromopyruvate and furfural show the strongest inhibition of PDH.
169 More importantly, effects of these inhibitors can be confirmed using a genetic
170 approach (i.e. comparison between a gene-specific mutant and an isogenic wild type
171 control). The inhibition of the conversion from pyruvate to AcCoA completely
172 abolished the glutamate-triggered killing effects, implying the critical role of the
173 alternative three steps and their effect on the TCA cycle.
174

175 **SI Materials and methods**

176 **Bacterial strains and culture conditions.**

The bacterial strains used in this study included *E. coli* K12 BW25113 and its gene-deleted mutants, which was obtained from NBRP (NIG, Japan), and seven other pathogens *E. coli, Vibrio anguillanum, V. alginolyticus, V. parahaemolyticus, V vulnificus, V. flurialis* and *Klebsiella pneumonia* from the collections of our laboratory. Bacterial culture conditions were essentially carried out as previously described (1, 8). Unless otherwise noted, frozen glycerol stocks were used to inoculate Luria-Bertani broth (LB) medium, supplemented with 50 μg/mL kanamycin for mutants, at 30 ^{0}C (*Vibrio* species) or 37 ^{0}C (*E. coli* and *K. pneumonia*) overnight. The cultures were diluted to 1:100 using fresh LB medium, or M9 medium (Na_2HPO_4 47.7 mM, KH_2PO_4 22 mM, NH_4Cl 18.7 mM, NaCl 8.6 mM, $MgSO_4$ 2 mM, $CaCl_2$ 0.1 mM) with 10 mM acetate plus 0.3% glucose or SOC medium and incubated overnight (24 h for *E. tarda* and 14 h for the others) at 200 r.p.m. and 80% humidity in 250 mL flasks or 20 mL tubes. Bacterial cells were collected by centrifugation at 8,000 g for 5 min in 4 ^{0}C. Followed by washing three times using sterile saline solution, bacterial cells were suspended in M9 medium with 10 mM acetate to arrive at 10^8 cells (*E. tarda*) or 5 $\times10^8$ (the others) or plus desired metabolites (or labeled) or/and antibiotics and cultured for 6 h (or 2h, or 4h for some isotope tracer experiments) in the same culture conditions. Harvested cells were used for GC-MS, plate counting and biochemical analysis.

GC-MS.

GC-MS analysis was carried out with a variation on the two-stage technique, the

resulting data were proceeded using pattern recognition methods, and the data matrix was normalized using internal control and the total peak area each strain as described previously (9, 10). Briefly, initial peak and mass spectral deconvolution were detected using MSD ChemStation (version EA. 02.02). Identification of metabolites was performed by the National Institute of Standards and Technology (NIST) library and NIST MS search 2.0 program. Using ribitol as the internal standard allowed normalization of the metabolites data. In the dataset the resulting normalized peak intensities formed a single matrix with Rt-m/z pairs for each file. This output file was used for further analysis.

Antibiotic bactericidal assays.

Antibiotic bactericidal assays were carried out as previously described (1, 8). Bacterial cells were collected as described above and suspended in M9 medium with 10 mM acetate, and in the presence or absence of 2.5 mM glutamate plus 30 and 500 μg/mL kanamycin for EIB202 and LTB4-R at 30 ^{0}C, respectively, and plus 1.2 μg/mL gentamicin for *E. coli* (*E. coli* K12 BW25113 gene-deleted mutants with kanamycin resistance) at 37 ^{0}C for 6 h. Otherwise, the desired antibiotic was indicated in the context. Percent survival was performed by serially diluted and spot-plated onto LB agar plates to determine colony-forming units (CFU) per mL and survival. Percentage of survival was determined by dividing the CFU obtained from a treated sample by the CFU obtained from control.

Isotope tracer.

The effects of $^{13}C_5$-labeled glutamate tracers on flux estimation precision were investigated as previously described (11, 12). In brief, EIB202 or *E. coli* K12 cells were harvested in LB medium, or in M9 medium with 10 mM acetate plus 0.3% glucose or in SOC medium, and then suspended in M9 medium with 10 mM acetate at 6 h, or harvested in LB medium and then in M9 medium with 10 mM acetate at 2 h or 4 h using 2.5 mM unlabeled compound glutamate or 1.25 mM [U-$^{13}C_5$] and 1.25 mM unlabeled substrate as control and test groups, respectively. When 10 mM unlabeled compound glucose or 5 mM [U-$^{13}C_6$] and 5 mM unlabeled substrate were used, *E. coli* K12 cells were harvested in LB medium and then suspended in M9 medium with 10 mM acetate at 6 h. Three biological replicates were performed each growth condition. GC-MS was performed using an Agilent 7890A GC equipped with a 30 m DB-35MS capillary column connected to an Agilent 5975C MS operating under electron impact (EI) ionization. The effectiveness of each tracer was gauged using the software downloaded from Internet (13). The software provides the mass isotopomer distributions (MID) data of all labeled compounds detected in the GC-MS data. Labeled compounds were identified from the MID data, which were used for estimation of metabolic fluxes. The estimation was carried out by the tracing of labeled atoms present in an externally supplied compound as it is metabolized. Both the spectrum obtained from the labeled chromatogram and the spectrum obtained from the unlabeled chromatogram was normalized by their total signal.

Ultra-performance liquid chromatography-MS/MS (UPLC-MS/MS).

Quantification of certain metabolite in bacteria by UPLC-MS/MS was carried out as previously described (14, 15). 10 mL bacteria suspension (OD_{600}=0.6) was collected, washed three times with 0.85% saline solution, and re-suspended in 1 mL of 50% acetonitrile (ACN). The bacteria were lysed with sonication. After centrifugation, supernatants were collected for UPLC-MS/MS analysis. UPLC was performed in Waters ACQUITY UPLC system equipped with an Acquity BEH C_{18} column (50 mm × 2.1 mm i.d., 1.7 μm; Waters Corp.). Metabolites were separated by linear gradient elution with mobile phase A (ACN) and B (0.1% formic acid in ultra-pure water) at a flow rate of 0.3 mL/min. The gradient elution was as follows: 0 - 0.5 min, 10% A; 0.5 - 1.2 min, 90% A; 1.2 - 3 min, 10 % A. The injection volume was 10 μL, and the column temperature was maintained at 35 ℃. Mass spectrometry detection was carried out with QUATTRO PREMIER XE equipped with an electrospray ionization source operating in negative ionization mode (ESI-). The capillary voltage was set to -3,000 V; the cone voltage was set to 10V. The extractor voltage and RF Lens were set at -3 V and -0.1 V, respectively. The desolvation gas flow was set to 650 L/h at temperature of 450 ℃, the cone gas flow rate was set at 50 L/h and the source temperature was set at 120 ℃.

Determination of NAD^+/NADH ratio.

The NAD^+/NADH ratio was measured with the EnzyChrom™ NAD/NADH assay kit (BioAssay Systems, USA) according to manufacturer's instructions. In brief, 1 mL of

bacterial suspension (OD_{600} = 0.6) was collected, resuspended in NAD^+ or NADH extraction buffer, and incubated at 60 ℃ for 5 min. The opposite extraction buffer (NADH extraction buffer was added for detection of NAD^+; NAD^+ extraction buffer was added for detection of NADH) was added to neutralize the extracts. Following vortex briefly, the neutralized extracts were centrifuged at 14,000 rpm for 5 min. Supernatants were collected for measurement of NAD^+ and NADH using the EnzyChrom™ NAD/NADH Assay Kit. Relative amounts of NAD^+ or NADH were determined by comparing the absorbance of the samples to a standard curve generated by the cycling assay performed on 0 to 10 μM of pure NAD^+. Optical density (OD0) for time "zero" and OD15 after a 15-min incubation were read at 565 nm (520-600nm) in room temperature. OD0 was subtracted from OD15 for the standard and sample wells. The ΔOD values were used to determine sample NAD^+/NADH concentration from the standard curve.

Quantification of intracellular adenosine nucleotides in bacteria.

To extract adenine nucleotides from bacteria, 2 mL of bacterial suspension (OD_{600} = 0.6) was collected and mixed immediately with 600 μL hot ethanol. The mixture was incubated at 80 ℃ for 10 min in hot-water bath. After cooling in ice, the volume was readjusted to 2 mL with cold solution buffer (50 mM tricine, 10 mM MgSO4, and 2 mM EDTA at pH7.8), followed by centrifugation to remove the denatured protein. To quantify intracellular concentration of ATP, ATP plus ADP and total adenosine nucleotides, 40 μL of the cell extract was added to the reaction buffer (75 mM tricine,

pH7.5; 5 mM $MgCl_2$, and 0.0125 mM KCl), reaction buffer supplemented with 0.5 mM phosphoenolpyruvate (Sigma) and 4 μg of pyruvate kinase (Sigma), and reaction buffer supplemented with 7.5 U of adenylate (myo) kinase (Sigma), respectively. The mixtures were incubated at 30 ℃ for 15 min. ATP was then determined with luciferin/luciferase using BacTiter-Glo™ Microbial Cell Viability Assay. Adenylate energy charge (AEC) was calculated as described by (ATP + 0.5 × ADP) / (ATP +ADP + AMP).

Membrane potential.

BacLight bacterial membrane potential kit (Invitrogen) was used to measure membrane potential. In brief, 1 mL of bacterial suspension (OD_{600} = 0.6) was collected and diluted to 10^6 CFU/mL and mixed immediately with 10 μL of 3 mM $DiOC_2(3)$ (3, 3'-diethyloxa-carbocyanine iodide). The mixture was incubated with oscillation at 37 ℃ for 30 min. Membrane potential was assessed by FACSCalibur flow cytometer (Becton Dickinson, San Jose, CA, USA). The green fluorescence was detected through a 488- to 530-nm bandwidth band-pass filter, and the red fluorescence was detected through a 488- to 610-nm bandwidth band-pass filter. The membrane potential was determined and normalized as the intensity ratio of the red/green fluorescence. The membrane potential was calculated with the following formula: $\mathrm{Log}(10^{3/2} \times (\frac{\text{red fluorescence}}{\text{green fluorescence}}))$.

ELISA assay for intracellular kanamycin and gentamicin.

309 Bacterial intracellular kanamycin and gentamicin were detected using ELISA rapid
310 diagnostic kit (Beijing Clover Technology Group Inc. Beijing, China). In brief,
311 samples were incubated in M9 medium with glutamate or/and an antibiotic for 6 h,
312 and collected by centrifugation at 8,000g for 5 min. The resulting pellets were washed
313 three times, re-suspended in sterile saline and adjusted to $OD_{1.0}$. Then 1 mL samples
314 were sonicated for 5 min and supernatant was for determination of antibiotic content.
315 Luminescence intensity was taken on a Perkin-Elmer LS55 Fluorescence
316 Spectrophotometer. The luminescence intensity was cuvette path length (10 mm)
317 quartz cell with excitation and emission spectra were recorded as 287 and 450 nm,
318 respectively. Kanamycin and gentamicin working standard solutions were from 0 to 3
319 ng/mL. The duplicate readings were averaged for each standard and zero standard
320 optical density 450 nm was subtracted. A standard curve was constructed by plotting
321 the mean absorbance for each standard on the y-axis against the concentration on the
322 x-axis, drawing the best fit curve, and then determining sample concentration from the
323 standard curve.
324
325 **Quantitative reverse-transcription PCR.**
326 Quantitative reverse-transcription PCR (qRT-PCR) was carried out as previously
327 described (16). Total RNA of each sample was isolated with Trizol (Invitrogen, USA).
328 The RNA was then quantified spectrophotometrically. The first-strand cDNA was
329 synthesized using a PrimeScriptTM RT reagent kit with gDNA eraser (TaKaRa). At
330 first, 1 μg of RNA extract was mixed with gDNA eraser and buffer at 42 ℃ for 2 min

in total volume of 10 μL mixture to remove genomic DNA (gDNA). Then, the mixture was used to synthesize cDNA according to the manufacturer's instructions. The reaction was carried out at 37 ℃ for 15 min, 85 ℃ for 5 sec. Real-time PCR was performed using specific primers in a LightCycle 480 system (Roche, Germany). Each sample was assayed in triplicate. Primers used for qRT-PCR were shown in **SI Appendix Table S9**. Reactions were performed in the LightCycle 480 system (Roche, Germany) according to the manufacturer's instructions. 10 μL reaction volumes containing 1 μL cDNA diluted with ddH_2O, 5 μL of 2 × SYBR-Green Master Mix (TaKaRa), and 400 nM of each primer. The cycling parameters were listed as follows: 95 ℃ for 30 s to activate the polymerase; 40 cycles of 95 ℃ for 10 s; 60 ℃ for 30 s. Fluorescence measurements were performed at 70 ℃ for 1 s during each cycle. Cycling was terminated at 95 ℃ with a calefactive velocity of 5 ℃/s to obtain a melting curve. To analyze the relative expression level of genes, we converted the data to percentages relative to the value of control group.

Enzyme assays.

Phosphoenolpyruvate carboxykinase / citrate synthase activity was determined using the enzymatic kit (Suzhou Comin Biotechnology Co., Ltd., Suzhou, China). The reaction started by the addition of 30 μg phosphoenolpyruvate carboxykinase or 50 μg citrate synthase. OAA concentration varied between 0.625 and 320 mM. Substrate saturation curves were fit to the Michaelis-Menten equation. The Michaelis-Menten constant (K_m) and the maximum velocity of the enzyme (V_{max}) were calculated from

353 the direct linear plot of Eisenthal and Cornish-Bowden (17). Isocitrate dehydrogenase
354 and α-ketoglutarate dehydrogenase activities were measured using Assay kits
355 (Genmed Scientifics Inc., USA). In brief, 24-h EIB202 cultures were diluted in M9
356 medium plus 10 mM acetate to an OD_{600} of 0.2 and then incubated in M9 medium
357 plus 10 mM acetate with an exogenous metabolite at 30 ^{0}C for 6 h. Cells were
358 collected, washed and resuspended in lysate (from the Assay kits), and disrupted by
359 intermittent sonic oscillation. Following centrifugation, supernatant was transferred to
360 new tube and used Bradford Assay to detect the protein concentrations. Then samples
361 were detected by Assay kits.
362
363 **Western blot**
364 Western blot was carried out as previously described (18). In brief, Bacterial protein
365 samples were separated in a 3% stacking gel (pH 6.8) and a 10% separating gel (pH
366 8.9) in Tris-glycine buffer (pH 8.3) and then transferred onto PVDF membranes for 6
367 h at 200 mA in transfer buffer (25 mM Tris, 0.1 M glycine and 20% methanol).
368 Membranes were blocked for 60 min with 5% skimmed milk in TBS (20 mM Tris,
369 150 mM NaCl, pH 7.4) at 37 ^{0}C, then incubated first with primary antibodies for 2 h
370 at 37 ^{0}C, followed by second antibody at 37 ^{0}C in TBST (20 mM Tris, 150 mM NaCl,
371 0.5% Tween-20, pH 7.4) containing 5% skimmed milk on a shaker. Band intensities
372 were detected by using a gel documentation system, LAS-3000 (Fujifilm Medical
373 systems, Stamford, USA).
374

Genetic complementation.

Genes *tdcE, aceE, lpdA, pykF, pflD* from *E. coli* K12 were amplified by PCR with primers as shown in **SI Appendix Table S10**. PCR products from *lpdA*, *pykF* and *pflD* were digested by restriction enzyme *Hind*III/*BamH*I, and cloned into the linearized plasmid pACYC184. PCR products from *tdcE* and *aceE* with flanking sequences which were homogenous with pACYC184 were purified and cloned into the linearized pACYC184 using ClonExpressTM II One Step Cloning kit (Vazyme Biotech Co. Ltd., Nanjing, China). Recombinant plasmids were checked by digestion with restriction endonucleases and electroporated into *E. coli* deletion cells.

References

1. Peng B, Su YB, Li H, Han Y, Guo C, Tian YM, Peng XX. (2015) Exogenous alanine or/and glucose plus kanamycin kills antibiotic-resistant bacteria. *Cell Metab* 21:249-261.
2. Mainguet SE, Gronenberg LS, Wong SS, Liao JC. (2013) A reverse glyoxylate shunt to build a non-native route from C4 to C2 in *Escherichia coli*. *Metab Eng* 19:116-127.
3. Grahl N, Demers EG, Lindsay AK, Harty CE, Willger SD, Piispanen AE, Hogan DA. (2015) Mitochondrial activity and Cyr1 are key regulators of Ras1 activation of *C. albicans* virulence pathways. *PLoS Pathog* 11:e1005133.
4. Asanuma N, Hino T. (2001) Molecular characterization, enzyme properties and transcriptional regulation of phosphoenolpyruvate carboxykinase and pyruvate

397 kinase in a ruminal bacterium, *Selenomonas ruminantium*. *Microbiology* 147(Pt
398 3):681-690.
399 5. Lowe PN, Perham RN. (1984) Bromopyruvate as an active-site-directed inhibitor
400 of the pyruvate dehydrogenase multienzyme complex from *Escherichia coli*.
401 *Biochemistry* 23:91-97.
402 6. Minato Y, Fassio SR, Häse CC. (2013) Malonate inhibits virulence gene
403 expression in *Vibrio cholerae*. *PLoS One* 8:e63336.
404 7. Modig T, Lidén G, Taherzadeh MJ. (2002) Inhibition effects of furfural on alcohol
405 dehydrogenase, aldehyde dehydrogenase and pyruvate dehydrogenase. *Biochem J*
406 363(Pt 3):769-776.
407 8. Allison KR, Brynildsen MP, Collins JJ. (2011) Metabolite-enabled eradication of
408 bacterial persisters by aminoglycosides. *Nature* 473:216-220.
409 9. Du CC, Yang MJ, Li MY, Yang J, Peng B, Li H, Peng XX. (2017) Metabolic
410 mechanism for L-Leucine-induced metabolome to eliminate *Streptococcus iniae*. *J*
411 *Proteome Res* 16:1880-1889.
412 10. Zeng ZH, Du CC, Liu SR, Li H, Peng XX, Peng B. (2017) Glucose enhances
413 tilapia against *Edwardsiella tarda* infection through metabolome reprogramming.
414 *Fish Shellfish Immunol* 61:34-43.
415 11. Hiller K, Metallo CM, Kelleher JK, Stephanopoulos G. (2010) Nontargeted
416 elucidation of metabolic pathways using stable-isotope tracers and mass
417 spectrometry. *Anal Chem* 82:6621-6628.
418 12. Hiller K, Wegner A, Weindl D, Cordes T, Metallo CM, Kelleher JK,

Stephanopoulos G. (2013) NTFD - a stand-alone application for the non-targeted detection of stable isotope-labeled compounds in GC/MS data. *Bioinformatics* 29:1226-1228.

13. Hiller K, Wegner A, Weindl D, Cordes T, Metallo CM, Kelleher JK, Stephanopoulos G. (2013) NTFD - a stand-alone application for the non-targeted detection of stable isotope-labeled compounds in GC/MS data. *Bioinformatics* 29:1226-1228.
14. Birkler RI, Støttrup NB, Hermannson S, Nielsen TT, Gregersen N, Bøtker HE, Andreasen MF, Johannsen M. (2010) A UPLC-MS/MS application for profiling of intermediary energy metabolites in microdialysis samples - a method for high-throughput. *J Pharm Biomed Anal* 53:983-990.
15. Rühl M, Rupp B, Nöh K, Wiechert W, Sauer U, Zamboni N. (2012) Collisional fragmentation of central carbon metabolites in LC-MS/MS increases precision of ^{13}C metabolic flux analysis. *Biotechnol Bioeng* 109:763-771.
16. Li WX, Yao ZJ, Sun LN, Hu WJ, Cao JJ, Lin WX, Lin XM. (2016) Proteomics analysis reveals a potential antibiotic cocktail therapy strategy for Aeromonas hydrophila infection in biofilm. *J Proteome Res* 15:1810-1820.
17. Eisenthal R, Cornish-Bowden A. (1974) The direct linear plot. A new graphical procedure for estimating enzyme kinetic parameters. *Biochem J* 139:715-720.
18. Zhang YL, Peng B, Li H, Yan F, Wu HK, Zhao XL, Lin XM, Min SY, Gao YY, Wang SY, Li YY, Peng XX. (2017) C-terminal domain of hemocyanin, a major antimicrobial protein from litopenaeus vannamei: Structural homology with

441 immunoglobulins and molecular diversity. *Frontires Immunol* 8:611.
442

Fig. S

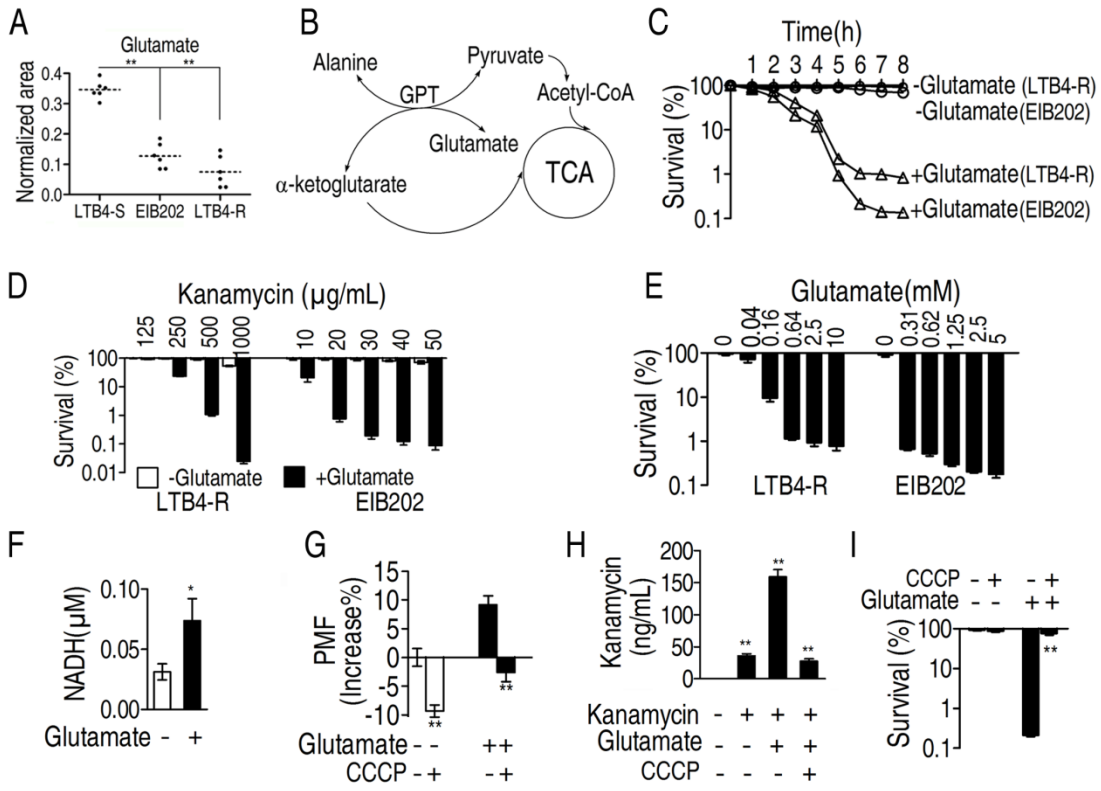

Fig. S1

Fig. S1. Glutamate restores susceptibility of drug-resistant *E. tarda* to kanamycin**.** (*A*) Glutamate content in the kanamycin-resistant *E. tarda* by GC-MS detection. Data were from Reference (11). (*B*) Metabolic pathways of alanine and glutamate to the TCA cycle. GPT, glutamic-pyruvic transaminase. (*C-E*) Percent survival of LTB4-R and EIB202 with increasing incubation periods (*C*), or increasing kanamycin (*D*) or increasing glutamate (*E*). Cells were grown in LB medium and then incubated in M9 medium plus acetate (10 mM) and glutamate (2.5 mM) and kanamycin (500 μg/mL and 30 μg/mL, respectively) for the indicated incubation periods (*C*), or for the indicated kanamycin concentrations for 6h (*D*). or for the indicated glutamate concentrations for 6 h (*E*). (*F*) Intracellular NADH of EIB202, Cells were grown in

458 LB medium and then incubated in M9 medium plus acetate (10 mM) with and without
459 glutamate (2.5 mM). (*G*) PMF of EIB202. Cells were grown in LB medium and then
460 incubated in M9 medium plus acetate (10 mM) with and without glutamate (2.5 mM)
461 in the presence or absence of CCCP (20 μM). (*H* and *I*) Intracellular kanamycin (*H*)
462 and percent survival (*I*) of EIB202. Cells were grown in LB medium and then
463 incubated in M9 medium plus acetate (10 mM) and kanamycin (30 μg/mL) with and
464 without glutamate (2.5 mM) or/and CCCP (20 μM). Results (*A. C - I*) are displayed as
465 mean ± SEM, and three biological repeats were carried out. Significant differences are
466 identified (*p < 0.05, **p < 0.01) as determined by Student's t test. p < 0.01 in
467 Results (*C-E*).
468
469
470

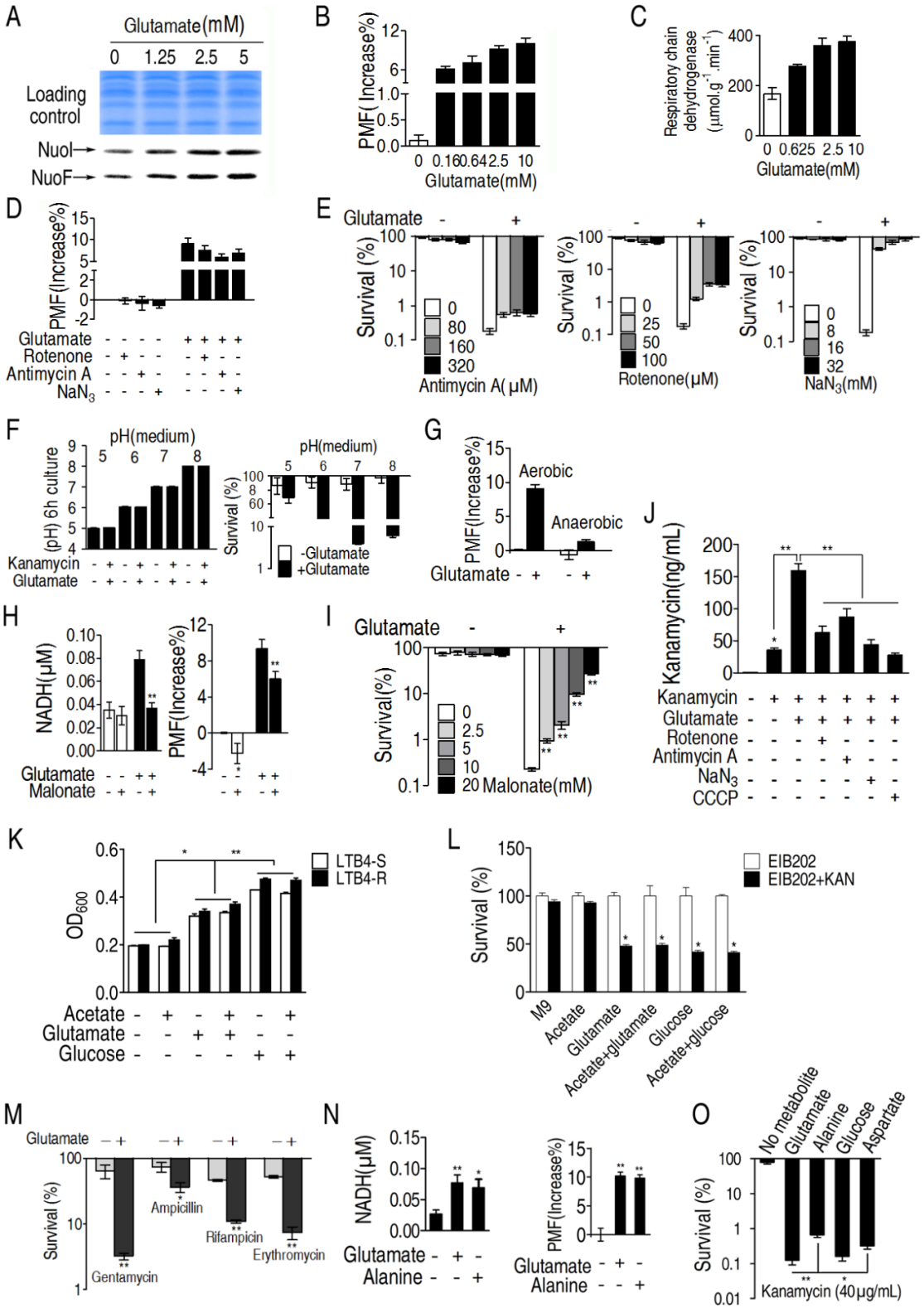

Fig. S2. Glutamate restores susceptibility to kanamycin and regulates NADH, PMF and cellular kanamycin. (*A-C*) Expression of NuoI and NuoF determined by Western blot (*A*), PMF (*B*) and activity of respiratory chain dehydrogenase (*C*) in EIB202.

Cells were grown in LB medium and then incubated in M9 medium plus acetate (10 mM) with and without the indicated concentrations of glutamate. (*D*) PMF of EIB202. Cells were grown in LB medium and then incubated in M9 medium plus acetate (10 mM) and in the presence or absence of glutamate (2.5 mM) and inhibitor rotenone (50 μM), antimycin A (80 μM) or NaN_3 (16 mM) effect. (*E*) Percent survival of EIB202. Cells were grown in LB medium and then incubated in M9 medium plus acetate (10 mM) and in the presence or absence of the increasing dosages of rotenone (50 μM), antimycin A (80 μM) or NaN_3 (16 mM) in the presence of glutamate (2.5 mM) and kanamycin (30 μg/mL). (*F*) Effect of environment pH on EIB202 growth (without kanamycin) (left) and percent survival (with 30 μg/mL kanamycin) (right). Cells were grown in LB medium and then incubated in M9 medium plus acetate (10 mM) in the presence or absence of glutamate (2.5 mM). (*G*) PMF of EIB202. Cells were grown in LB medium and then incubated in M9 medium plus acetate (10 mM) and in the presence or absence of glutamate (2.5 mM) under aerobic or anaerobic conditions. (*H*) NADH and PMF of EIB202. Cells were grown in LB medium and then incubated in M9 medium plus acetate (10 mM) in the presence or absence of glutamate (2.5 mM), and effect of malonate (20 mM). (*I*) Percent survival of EIB202. Cells were grown in LB medium and then incubated in M9 medium with acetate (10 mM) in the presence or absence of glutamate (2.5 mM) and effect of the indicated concentrations of malonate plus kanamycin (30 μg/mL). (*J*) Effect of glutamate (2.5 mM), rotenone (50 μM), antimycin A (80 μM), NaN_3 (16 mM) and/or CCCP (20 μM) on intracellular kanamycin. Cells were grown in LB medium and then incubated in M9 medium with

acetate (10 mM) plus kanamycin (30 μg/mL). (*K*) OD value of LTB4-S and LTB4-R. Cells were grown in LB medium and then incubated in M9 medium or plus the indicated metabolites acetate (10 mM), glutamate (2.5 mM), acetate (10 mM) and glutamate (2.5 mM), glucose (10 mM), or acetate (10 mM) and glucose (10 mM) for 6 h. (*L*) Percent survival of nongrowing EIB202. Cells were grown in LB medium. The cultures incubated in M9 medium or plus acetate (10 mM) for 24 h. The resulting cells were incubated in M9 medium or plus acetate (10 mM), respectively, or the cells cultured in M9 medium plus acetate (10 mM) were incubated in M9 medium with glutamate (2.5 mM), or acetate (10 mM) and glutamate (2.5 mM), or glucose (10 mM), or acetate (10 mM) and glucose (10 mM) in the presence or absence of kanamycin (30 μg/mL). (*M*) Percent survival of EIB202. Cells were grown in LB medium and then incubated in M9 medium with acetate (10 mM) in the presence or absence of glutamate (2.5 mM) plus gentamicin (8 μg/mL), ampicillin (160 μg/mL), rifampicin (100 μg/mL) or erythromycin (6.4 mg/mL). (*N*) NADH (left) and PMF (right) of EIB202. Cells were grown in LB medium and then incubated in M9 medium with acetate (10 mM) in the presence or absence of glutamate (2.5 mM) or alanine (40 mM). (*O*) Percent survival of EIB202. Cells were grown in LB medium and then incubated in M9 with acetate (10 mM) in the presence or absence of glutamate (2.5mM), alanine (40mM), glucose (10 mM) or aspartate (10 mM) plus kanamycin (40 μg/mL). Results (*B* - *O*) are displayed as mean ± SEM, and three independent biological repeats were carried out. Significant differences are identified (*$p < 0.05$, **$p < 0.01$) as determined by Student's t test.

519

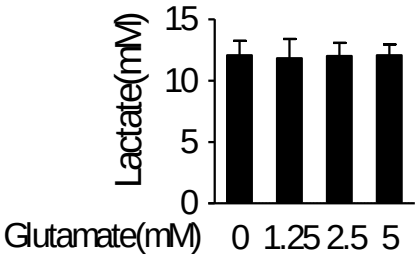

520

521 **Fig. S3.** Lactate measurement. EIB202 cells were grown in LB medium and then

522 incubated in M9 with acetate (10 mM) in the presence or absence of glutamate (2.5

523 mM)

524

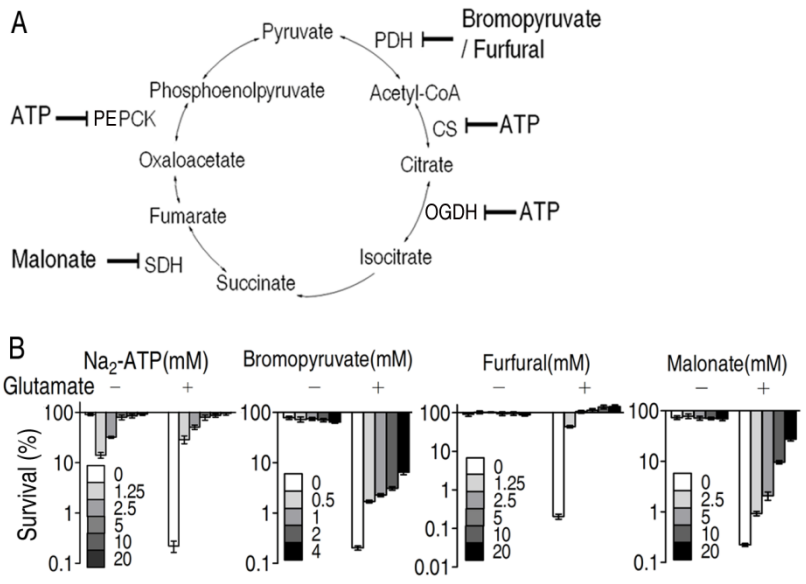

Fig. S4. Effect of inhibitors on the P cycle. (*A* and *B***)** Two other inhibitors - 1) furfural, a non-competitive inhibitor for PDH (pyruvate dehydrogenase), and - 2) Na_2-ATP, an inhibitor for PEPCK (phosphoenolpyruvate carboxykinase), CS (citrate synthase), IDH (isocitrate dehydrogenase), and OGDH (α-oxoglutarate dehydrogenase) - were used to further define the role of the three distinguishing steps of the P cycle (*A*). All of these inhibitors showed strong inhibition of glutamate-triggered killing effects, regardless of which cycle these enzymes belong to, and they did not affect the growth of EIB202. Furfural inhibited glutamate-mediated killing most efficiently while the other compounds inhibited the killing promoted by glutamate (2.5 mM) and kanamycin (30 μg/mL), in a dose-dependent manner (*B*). Cells were grown in LB medium and then incubated in M9 with acetate (10 mM) in the presence or absence of glutamate (2.5 mM) plus the indicated inhibitors. Results (*B*) are displayed as mean ± SEM, and three biological repeats were carried out. Significant differences are determined by Student's t test. All are $p < 0.01$.

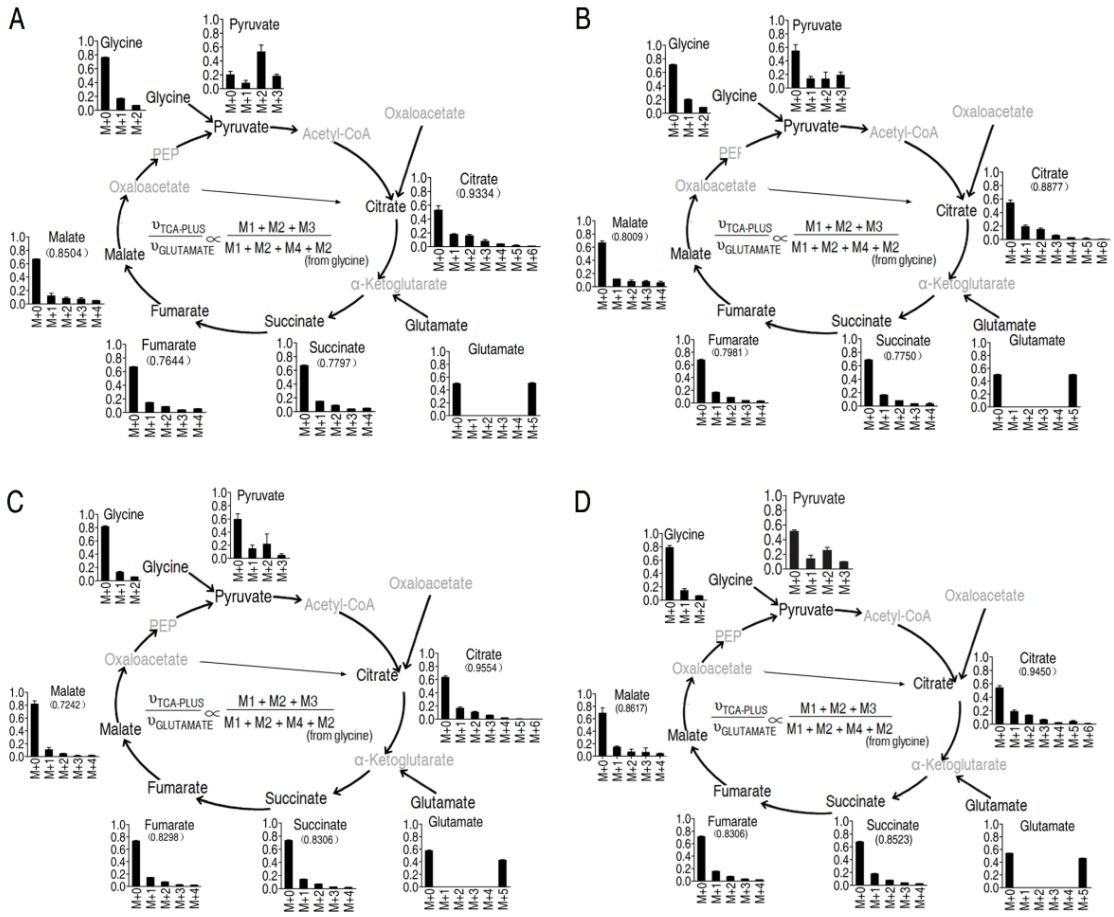

Fig. S5. Mass isotopomer analysis for ^{13}C labeled glutamate detected in a nontargeted manner in *E. coli* K12 cultured in different culture conditions. (*A*), Mass isotopomer distributions in the P cycle of *E. coli* K12. Cells were grown M9 medium with acetate (10 mM) plus 0.3% glucose and then incubated in M9 medium with acetate (10 mM) plus ^{13}C labeled glutamate (1.25 mM) and unlabeled glutamate (1.25 mM) at 6h. (*B*), Mass isotopomer distributions in the P cycle of *E. coli* K12. Cells were grown in SOC medium and then incubated in M9 medium with acetate (10 mM) plus ^{13}C labeled glutamate (1.25 mM) and unlabeled glutamate (1.25 mM) at 6h. (*C*), Mass isotopomer distributions in the P cycle of *E. coli* K12. Cells were cultured in LB medium and then incubated in M9 medium with acetate (10 mM) plus ^{13}C labeled glutamate (1.25 mM) and unlabeled glutamate (1.25 mM) at 2h. (*D*), Mass isotopomer distributions in the P

553 cycle of *E. coli* K12. Cells were cultured in LB medium and then incubated in M9

554 medium with acetate (10 mM) plus ^{13}C labeled glutamate (1.25 mM) and unlabeled

555 glutamate (1.25 mM) at 4 h. Each dot shows a biological or technical replicate.

556

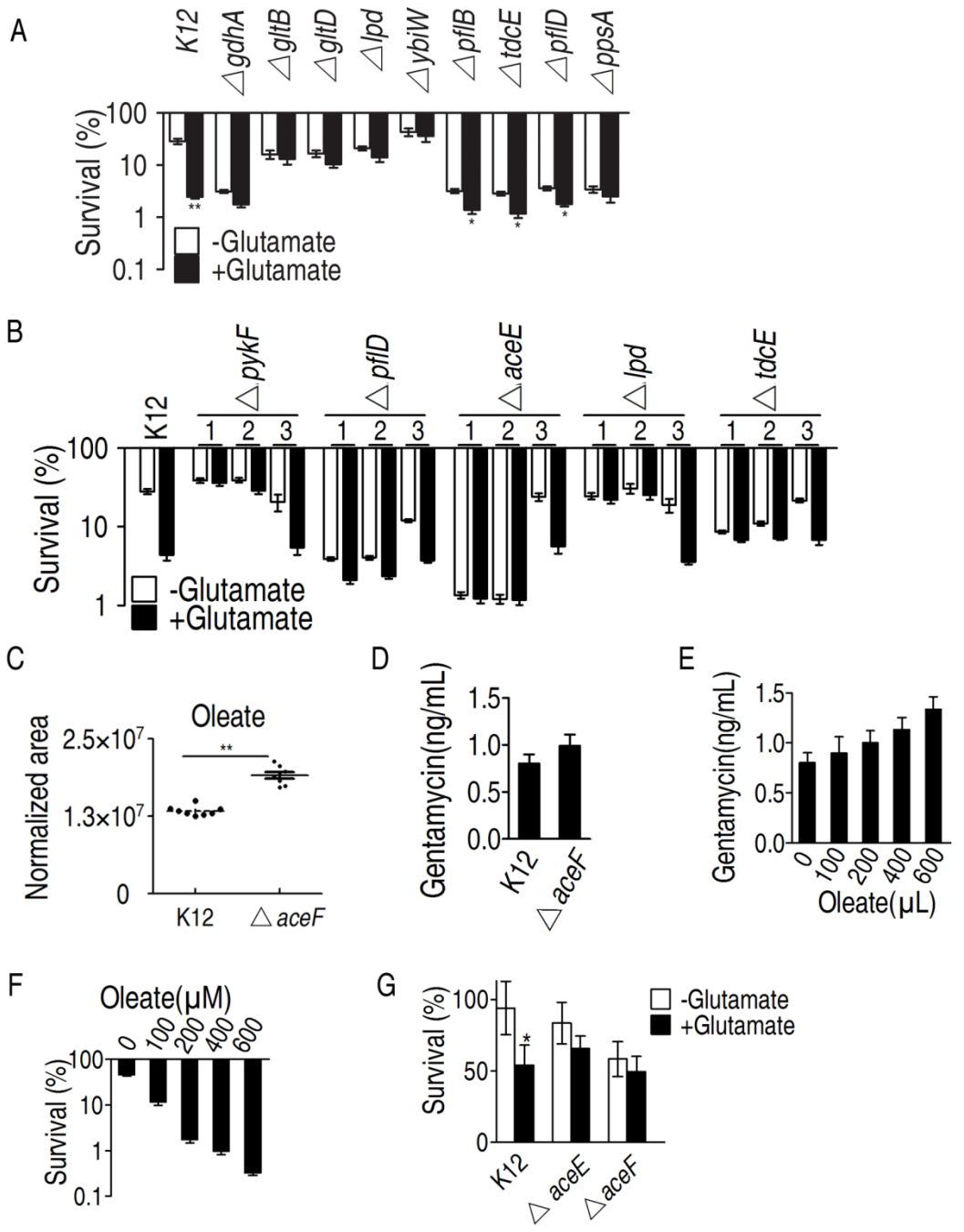

Fig. S6. Percent survival of rescued strains and oleate-enabled killing of *E. coli* K12 by gentamicin. (*A*) Percent survival of *E. coli* K12 and selected P cycle mutants. Cells were grown in LB medium and then incubated in M9 with acetate (10 mM) in the presence or absence of glutamate (2.5 mM) plus gentamicin (1.2 μg/mL). (*B*), Percent survival of rescued strains. 1, Mutant; 2, Plus plasmid pACYC184; 3, Plus plasmid pACYC184 + gene in the presence or absence of glutamate (2.5 mM) plus gentamicin

(1.2 μg/mL). (*C*-*F*) Oleate-enabled inactivation of *E. coli* K12 by gentamicin. Oleate level of *E. coli* K12 and Δ*aceF*, which was determined by GC-MS detection. (*C*) Intracellular concentration of gentamicin of *E. coli* K12 and Δ*aceF* with the presence of 1.2 μg/mL gentamicin (*D*). Intracellular gentamicin concentration in the presence of the indicated concentration of oleate with the presence of 1.2 μg/mL gentamicin (*E*). Percent survival of *E. coli* K12 in the presence of oleate plus gentamicin (0.75 μg/mL) (*F*). Cells were grown in LB medium and then incubated in M9 with acetate (10 mM) plus the indicated oleate or/and gentamicin. (*G*), Mouse urinary tracts were catheterized and infected with *E. coli* K12 and its mutants Δ*aceE* and Δ*aceF* with glutamate (250 mg/kg) and gentamicin (2 mg/kg). Results (*A* - *G*) are displayed as mean ± SEM, and three biological repeats were performed. Significant differences are identified (*p < 0.05, **p < 0.01; **p < 0.01 was detect in *E* and *F*) as determined by Student's t test.

Tables S

Table S1. Summary of all compounds being detected as labeled by the [U-^{13}C] labeled L-glutamate in *E. tarda* EIB202, which were cultured in LB medium and then incubated in M9 plus acetate with the labeled glutamate

RT	Name	Fragments	Pathway
7.45	Alanine	3	Alanine,aspartate and glutamate metabolism
9.16	Butanoate	4	Butanoate metabolism
9.56		2	
10.27	L-Valine	1	Valine, leucine and isoleucine biosynthesis
11.23		3	
12.86	Succniate	4	TCA cycle
13.42	Uracil	4	Pyrimidine metabolism
13.80	Fumarate	4	TCA cycle
14.31	α-D-Glucopyranoside	1	
14.69	L-threonine	3	Glycine, serine and threonine metabolism
15.01		4	
16.01	L-Homoserine	3	Glycine, serine and threonine metabolism
16.22		3	
17.26	Malate	3	TCA cycle
18.03	L-Proline	6	Arginine and proline metabolism
18.29		5	
19.35	Pentanedioic acid	4	L-Lysine degradation
19.83	2-Propenoic acid	3	Styrene degradation
20.09		3	
20.38	Glutamate	1	Alanine,aspartate and glutamate metabolism
21.38		5	
24.34		1	
24.67	Citrate	3	TCA cycle
24.98	Cadaverine	1	Glutathione metabolism
25.97	Tyrosine	3	Tyrosine metabolism
26.58		5	
26.93		6	
27.73		4	
29.88		5	
30.18	Oleic acid	6	Fatty acid biosynthesis
30.45		1	
30.86	Hexadecanoic acid	1	Fatty acid biosynthesis
31.31	9,12,15-Octadecatrienoic acid	2	Biosynthesis of unsaturated fatty acids
35.07		6	
35.17		2	
38.54	Glycine	1	Glycine, serine and threonine metabolism
40.22		1	
42.73		3	

585

586 **Table S2. Non-targeted detection of [U-^{13}C] labeled L-glutamate in *E. tarda***

587 **EIB202, which were cultured in LB medium and then incubated in M9 plus**

588 **acetate with the labeled glutamate**

Glutamate(^{13}C) RT	Name	Frag	R^2	M+0		M+1		M+2		M+3		M+4		M+5		M+6	
				100%	SD	100%	SD	100%	SD	100%	SD	100%	SD	100%	SD	100%	SD
7.45	Alanine	116	1	0.5797	0.0102	0.3094	0.0080	0.0846	0.0047	0.0279	0.0013						
12.86	Succniate	247	1	0.6740	0.0118	0.1434	0.0048	0.0791	0.0028	0.0263	0.0039	0.0780	0.0019				
13.8	Fumarate	245	1	0.6773	0.0097	0.1434	0.0051	0.0790	0.0014	0.0280	0.0038	0.0737	0.0012				
17.26	Malate	233	1	0.6974	0.0081	0.1633	0.0038	0.0647	0.0043	0.0706	0.0053	0.0057	0.0039				
20.38	Glutamate	246	1	0.5285	0.0275	0.0007	0.0007	0.0169	0.0435	0.0104	0.0094	0.0001	0.0127	0.4740	0.0344		
24.67	Citrate	273	1	0.5452	0.0326	0.2163	0.0214	0.1227	0.0246	0.0715	0.0116	0.0113	0.0035	0.0090	0.0026	0.0006	0.0020
26.9318	Hexadecanoic acid	123	1	0.9410	0.0118	0.0493	0.0048	0.0079	0.0025	0.0020	0.0021	0.0007	0.0011	0.0004	0.0008		
30.1785	Oleic acid	242	1	0.4456	0.0340	0.2193	0.0123	0.1024	0.0192	0.0504	0.0064	0.0942	0.0170	0.0387	0.0029	0.0124	0.0018
31.3143	9,12,15-Octadecatrienoic acid	57	1	0.6141	0.0661	0.2858	0.0611	0.0374	0.0435	0.0858	0.0382	0.0305	0.0224	0.0048	0.0076		

589

590

591 **Table S3.** Non-targeted detection of [U-^{13}C] labeled L-glutamate in *E. coli* K12

592 BW25113, which were cultured in LB medium and then in M9 medium plus acetate

593 with the labeled glutamate

Glutamate(^{13}C) RT	Name	Frag	R^2	M+0 M+7 100%	SD	M+1 M+8 100%	SD	M+2 M+9 100%	SD	M+3 M+10 100%	SD	M+4 100%	SD	M+5 100%	SD	M+6 100%	SD
7.85	Alanine	116	1	0.8063	0.0020	0.1382	0.0063	0.0425	0.0033	0.0130	0.0010						
12.70	Isoleucine	85	1	0.6008	0.0740	0.0705	0.0166	0.1544	0.0219	0.0328	0.0289	0.0531	0.0267	0.0318	0.0127	0.0566	0.0004
12.83	Proline	148	1	0.5753	0.0155	0.2412	0.0270	0.1113	0.0249	0.0158	0.0020	0.0283	0.0235	0.0282	0.0079		
13.01	Glycine	248	1	0.8935	0.0209	0.1077	0.0252	0.0030	0.0017								
13.32	Succniate	172.247	1	0.7648	0.0112	0.0704	0.0010	0.0547	0.0137	0.0407	0.0038	0.0439	0.0024				
13.88	Uracil	85	1	0.5977	0.0469	0.2410	0.0334	0.1153	0.0023	0.0264	0.0141	0.0195	0.0029				
14.25	Fumarate	79.245	1	0.7648	0.0112	0.0704	0.0010	0.0547	0.0137	0.0407	0.0038	0.0439	0.0024				
14.93	Citrate	347	1	0.6656	0.0339	0.1617	0.0400	0.1023	0.0305	0.0346	0.0098	0.0208	0.0175	0.0138	0.0045	0.0012	0.0017
15.09	Threonine	160	1	0.5732	0.0048	0.2506	0.0032	0.0409	0.0150	0.0987	0.0335	0.0365	0.0104				
17.68	Malate	119.233	1	0.8007	0.0720	0.0825	0.0011	0.0534	0.0010	0.0507	0.0023	0.0472	0.0036				
20.80	Glutamate	246	1	0.5073	0.5220	0.0000	0.0000	0.0000	0.0000	0.0000	0.0000	0.0000	0.0000	0.4927	0.4780		
24.18	Glutamine	116	1	0.6288	0.0100	0.2264	0.0143	0.0779	0.0117	0.0369	0.0116	0.0112	0.0073	0.0187	0.0116		
27.49	Tyrosine	280,354	1	0.5324	0.0197	0.2401	0.0143	0.1096	0.0010	0.0699	0.0025	0.0279	0.0054	0.0147	0.0032	0.0032	0.0001
32.67	Oleic acid	264	1	0.6475 0.0407	0.0145 0.0229	0.0853 0.0408	0.0033 0.0009	0.0127 0.0154	0.0064 0.0070	0.0366 0.0121	0.0173 0.0127	0.0163	0.0135	0.0410	0.0374	0.0222	0.0078

594
595
596

Table S4. Non-targeted detection of [U-^{13}C] labeled L-glutamate in *E. coli* K12 BW25113, which were cultured in M9 medium with acetate plus 0.3% glucose and then incubated in M9 medium plus acetate with the labeled glutamate

Glutamate(^{13}C) RT	Name	Frag	R^2	M+0 100%	SD	M+1 100%	SD	M+2 100%	SD	M+3 100%	SD	M+4 100%	SD	M+5 100%	SD	M+6 100%	SD
7.85	Alanine	116	1	0.7165	0.0062	0.1966	0.0038	0.0690	0.0023	0.0178	0.0002						
12.70	Isoleucine	158	1	0.6011	0.0088	0.2130	0.0016	0.0987	0.0060	0.0601	0.0038	0.0180	0.0015	0.0074	0.0010	0.0017	0.0002
12.83	Proline	148	1	0.5934	0.0034	0.1717	0.0023	0.0752	0.0007	0.0550	0.0018	0.0201	0.0001	0.0846	0.0012		
13.01	Glycine	248	1	0.7616	0.0049	0.1697	0.0035	0.0687	0.0014								
13.32	Succiniate	172.247	1	0.6695	0.0077	0.1505	0.0011	0.0910	0.0033	0.0392	0.0012	0.0498	0.0033				
13.88	Uracil	85	1	0.6225	0.0050	0.2123	0.0052	0.1101	0.0135	0.0246	0.0033	0.0305	0.0061				
14.25	Fumarate	79.245	1	0.6707	0.0048	0.1479	0.0017	0.0885	0.0023	0.0384	0.0008	0.0545	0.0034				
14.93	Citrate	347	1	0.5305	0.0627	0.1772	0.0107	0.1568	0.0197	0.0776	0.0250	0.0383	0.0035	0.0161	0.0091	0.0080	0.0013
15.09	Threonine	160	1	0.6028	0.0241	0.1469	0.0221	0.1092	0.0152	0.0994	0.0421	0.0417	0.0196				
17.68	Malate	119.233	1	0.6702	0.0052	0.1219	0.0388	0.0839	0.0190	0.0719	0.0236	0.0521	0.0014				
20.80	Glutamate	246	1	0.4964	0.0096	0.0000	0.0000	0.0000	0.0000	0.0000	0.0000	0.0000	0.0000	0.5036	0.0096		
24.18	Glutamine	116	1	0.5612	0.0056	0.2302	0.0050	0.1122	0.0092	0.0472	0.0043	0.0149	0.0043	0.0343	0.0045		
27.49	Tyrosine	280,354	1	0.4891	0.0122	0.2197	0.0031	0.1431	0.0057	0.0887	0.0058	0.0361	0.0028	0.0140	0.0007	0.0056	0.0002
32.67	Oleic acid	264	1	0.3812	0.0270	0.0747	0.0028	0.0818	0.0094	0.0481	0.0078	0.0528	0.0072	0.0169	0.0033	0.0118	0.0039
				0.0052(M+7)	0.0003	0.0050(M+8)	0.0014	0.0039(M+9)	0.0039	0.0116(M+10)	0.0046						

602 **Table S5.** Non-targeted detection of [U-^{13}C] labeled L-glutamate in *E. coli* K12

603 BW25113, which were cultured in SOC medium and then incubated in M9 medium

604 plus acetate with the labeled glutamate

Glutamate(^{13}C) RT	Name	Frac	R^2	M+0 100%	SD	M+1 100%	SD	M+2 100%	SD	M+3 100%	SD	M+4 100%	SD	M+5 100%	SD	M+6 100%	SD
7.85	Alanine	116	1	0.7030	0.0013	0.2036	0.0032	0.0741	0.0009	0.0193	0.0020						
12.70	Isoleucine	158	1	0.6845	0.0142	0.1875	0.0077	0.0717	0.0035	0.0385	0.0024	0.0117	0.0009	0.0046	0.0007	0.0015	0.0004
12.83	Proline	148	1	0.5826	0.0087	0.1984	0.0018	0.0902	0.0021	0.0555	0.0013	0.0190	0.0007	0.0543	0.0049		
13.01	Glycine	248	1	0.7132	0.0080	0.2017	0.0066	0.0850	0.0028								
13.32	Succiniate	172.247	1	0.6858	0.0082	0.1647	0.0054	0.0811	0.0016	0.0359	0.0009	0.0326	0.0162				
13.88	Uracil	85	1	0.6855	0.0172	0.1753	0.0134	0.0951	0.0103	0.0173	0.0047	0.0269	0.0101				
14.25	Fumarate	79.245	1	0.6781	0.0098	0.1658	0.0072	0.0868	0.0027	0.0383	0.0012	0.0310	0.0023				
14.93	Citrate	347	1	0.5437	0.0402	0.1920	0.0223	0.1512	0.0195	0.0621	0.0070	0.0283	0.0031	0.0154	0.0106	0.0047	0.0035
15.09	Threonine	160	1	0.5954	0.0084	0.2529	0.0144	0.0551	0.0092	0.0719	0.0034	0.0247	0.0003				
17.68	Malate	119.233	1	0.6664	0.0287	0.1169	0.0012	0.0788	0.0231	0.0775	0.0163	0.0604	0.0207				
20.80	Glutamate	246	1	0.4996	0.0083	0.0000	0.0000	0.0000	0.0000	0.0000	0.0000	0.0000	0.0000	0.5004	0.0083		
27.49	Tyrosine	280.354	1	0.5285	0.0193	0.2112	0.0122	0.1281	0.0052	0.0769	0.0110	0.0350	0.0045	0.0140	0.0040	0.0064	0.0038

605

606

607

608 **Table S6. Non-targeted detection of [U-^{13}C] labeled L-glutamate at 2 h in *E.***

609 ***coli* K12 BW25113, which were cultured in LB medium and then incubated in**

610 **M9 medium plus acetate with the labeled glutamate**

Glutamate(^{13}C) RT	Name	Frag	R^2	M+0 100%	SD	M+1 100%	SD	M+2 100%	SD	M+3 100%	SD	M+4 100%	SD	M+5 100%	SD	M+6 100%	SD
7.85	Alanine	116	1	0.7589	0.0068	0.1771	0.0061	0.0484	0.0028	0.0157	0.0023						
13.01	Glycine	248	1	0.8159	0.0115	0.1278	0.0127	0.0563	0.0023								
13.32	Succniate	172.247	1	0.7350	0.0094	0.1445	0.0031	0.0718	0.0030	0.0277	0.0015	0.0211	0.0022				
13.88	Uracil	85	1	0.6667	0.0272	0.1801	0.0236	0.0986	0.0217	0.0179	0.0050	0.0367	0.0157				
14.25	Fumarate	79.245	1	0.7329	0.0101	0.1437	0.0026	0.0733	0.0034	0.0281	0.0020	0.0220	0.0023				
14.93	Citrate	347	1	0.6360	0.0200	0.1660	0.0202	0.1070	0.0114	0.0613	0.0043	0.0206	0.0015	0.0068	0.0020	0.0023	0.0008
15.09	Threonine	160	1	0.6522	0.0816	0.1246	0.0184	0.1381	0.0764	0.0772	0.0205	0.0080	0.0385				
17.68	Malate	119.233	1	0.8195527	0.050317973	0.1066674	0.034779414	0.044477	0.005986731	0.011781035	0.009807	0.017521875	0.00567547				
20.80	Glutamate	246	1	0.5748	0.0109	0.0000	0.0000	0.0000	0.0000	0.0000	0.0000	0.0000	0.0000	0.4252	0.0109		
24.18	Glutamine	116	1	0.4178	0.0609	0.1153	0.0278	0.0644	0.0224	0.0285	0.0179	0.0178	0.0034	0.0260	0.0225		

611

612

Table S7. Non-targeted detection of [U-^{13}C] labeled L-glutamate at 4h in *E. coli* K12 BW25113, which were cultured in LB medium and then incubated in M9 medium plus acetate with the labeled glutamate

Glutamate(^{13}C) RT	Name	Frag	R^2	M+0 100%	SD	M+1 100%	SD	M+2 100%	SD	M+3 100%	SD	M+4 100%	SD	M+5 100%	SD	M+6 100%	SD
7.85	Alanine	116	1	0.7002	0.0386	0.2173	0.0239	0.0670	0.0083	0.0155	0.0082						
12.70	Isoleucine	158	1	0.7798	0.0140	0.1494	0.0111	0.0444	0.0034	0.0177	0.0021	0.0047	0.0006	0.0022	0.0026	0.0018	0.0007
12.83	Proline	148	1	0.2645	0.0583	0.1251	0.2976	0.2172	0.2369	0.1333	0.0925	0.0767	0.0503	0.1831	0.0769		
13.01	Glycine	248	1	0.7896	0.0294	0.1455	0.0271	0.0649	0.0047								
13.32	Succniate	172,247	1	0.6756	0.0087	0.1796	0.0058	0.0798	0.0004	0.0391	0.0013	0.0259	0.0018				
13.88	Uracil	85	1	0.6895	0.0273	0.1671	0.0278	0.0965	0.0067	0.0230	0.0054	0.0239	0.0090				
14.25	Fumarate	79,245	1	0.7115	0.0104	0.1566	0.0048	0.0751	0.0043	0.0338	0.0017	0.0231	0.0001				
14.93	Citrate	347	1	0.5396	0.0324	0.1883	0.0215	0.1340	0.0050	0.0657	0.0076	0.0234	0.0016	0.0404	0.0124	0.0085	0.0062
15.09	Threonine	160	1	0.6131	0.0185	0.1612	0.0408	0.0718	0.0340	0.1319	0.0218	0.0220	0.0182				
17.68	Malate	119,233	1	0.6889	0.0868	0.1468	0.0154	0.0665	0.0448	0.0594	0.0728	0.0384	0.0092				
20.80	Glutamate	246	1	0.5400	0.0042	0.0000	0.0000	0.0000	0.0000	0.0000	0.0000	0.0000	0.0000	0.4600	0.0042		
24.18	Glutamine	116	1	0.6924	0.0252	0.1688	0.0104	0.0745	0.0052	0.0434	0.0153	0.0127	0.0153	0.0081	0.0048		
27.49	Tyrosine	280,354	1	0.5592	0.0264	0.1885	0.0237	0.1218	0.0099	0.0575	0.0009	0.0278	0.0064	0.0180	0.0047	0.0138	0.0125

Table S8. Non-targeted detection of [U-^{13}C] labeled L-glucose in *E. coli* K12 BW25113, which were cultured in LB medium and then incubated in M9 medium plus acetate with the labeled glucose

Glucose(^{13}C) RT	Name	Frag	R^2	M+0 100%	SD	M+1 100%	SD	M+2 100%	SD	M+3 100%	SD	M+4 100%	SD	M+5 100%	SD	M+6 100%	SD
7.85	Alanine	116	1	0.6672	0.0065	0.1644	0.0024	0.1498	0.0078	0.0186	0.0009						
12.70	Isoleucine	158	1	0.6561	0.0044	0.1560	0.0029	0.1201	0.0002	0.0444	0.0010	0.0167	0.0007	0.0057	0.0006	0.0009	0.0000
12.83	Proline	148	1	0.6030	0.0173	0.1750	0.0041	0.1133	0.0030	0.0372	0.0015	0.0120	0.0012	0.0595	0.0128		
13.01	Glycine	248	1	0.7304	0.0111	0.2049	0.0144	0.0647	0.0126								
13.32	Succniate	172,247	1	0.4912	0.0055	0.2346	0.0009	0.1441	0.0011	0.0986	0.0024	0.0314	0.0014				
13.88	Uracil	85	1	0.5534	0.0079	0.2232	0.0023	0.1298	0.0017	0.0719	0.0038	0.0216	0.0022				
14.25	Fumarate	79,245	1	0.5337	0.0068	0.2134	0.0030	0.1315	0.0020	0.0905	0.0027	0.0309	0.0025				
14.93	Citrate	347	1	0.4240	0.0359	0.2237	0.0217	0.1938	0.0128	0.0974	0.0088	0.0356	0.0044	0.0136	0.0006	0.0115	0.0042
15.09	Threonine	160	1	0.5665	0.0150	0.2013	0.0070	0.1444	0.0112	0.0619	0.0031	0.0259	0.0005				
17.68	Malate	119,233	1	0.5419	0.0133	0.2200	0.0052	0.1467	0.0030	0.0755	0.0057	0.0159	0.0010				
20.80	Glutamate	246	1	0.5332	0.0021	0.1594	0.0020	0.0661	0.0003	0.0212	0.0002	0.0212	0.0002	0.0043	0.0001		
24.18	Glutamine	116	1	0.5036	0.0275	0.2133	0.0140	0.1597	0.0076	0.0735	0.0120	0.0385	0.0120	0.0114	0.0051		
27.49	Tyrosine	280,354	1	0.3377	0.0211	0.1497	0.0068	0.1897	0.0089	0.1426	0.0064	0.0896	0.0088	0.0488	0.0059	0.0255	0.0051
				0.0098 (M+7)	0.0012	0.0053 (M+8)	0.0019	0.0013 (M+9)	0.0008								

627 **Table S9 Primers used for QRT-PCR**

628

A: *Escherichia coli*

Gene	Primer	Primer sequence	Product size(bp)
16SrRNA	Forward	5'-ACTGAGACACGGTCCAGACTCCTAC-3'	146
	Reverse	5'-TTAACGTTCACACCTTCCTCCCTAC-3'	
pck	Forward	5'-GATGAACGGAGCCAAATGCA-3'	239
	Reverse	5'-GGCCAAAGAAGATCGCCAC-3'	
pykF	Forward	5'-TTCACCACCGACCAGAGCG-3'	112
	Reverse	5'-TCAGGCCATCGTCCACCAG-3'	
aceE	Forward	5'-ACCTCTGGACGCACCACCCT-3'	181
	Reverse	5'-AGTACACGTTCTCCTGCTTCTCA-3'	
aceF	Forward	5'-CAGGGCGGCTGCTTCACTA-3'	141
	Reverse	5'-CGCAAACTCTTTCCCATTCCA-3'	
gltA	Forward	5'-TGAGCTGGGTATGAATGACGA-3'	127
	Reverse	5'-CAGTATGATGCCGGAGTAGAAG-3'	
acnB	Forward	5'-TCCCTGTGCATGGGCAACC-3'	194
	Reverse	5'-CCCACCTTCGCCATAAACTGC-3'	
icd	Forward	5'-AAACGCCGAGGATATTTACGC-3'	126
	Reverse	5'-ATGCCGCAGTGCTCAGGGA-3'	
sucA	Forward	5'-ACCTACTGCGGAACCATCGG-3'	119
	Reverse	5'-TTCTCCTGCGGGCTAAACG-3'	
sucC	Forward	5'-GCCGAACAGTGGCTGGGTA-3'	89
	Reverse	5'-GTCGCTCCCTCCACCAGAAT-3'	
sdhA	Forward	5'-ACCCGTTCCCATACCGTTTC-3'	80
	Reverse	5'-TGCCATTCCCAGTTGTCTTCAT-3'	
frdA	Forward	5'-GCTGTCCGTGGAGCCGTAA-3'	81
	Reverse	5'-CAAACCAGGTGCGTTCAATCT-3'	
fumC	Forward	5'-GCCGTATGGACTCCTATGTCG-3'	177
	Reverse	5'-TCAGGCTCTTGATGCTCTGC-3'	
mdh	Forward	5'-ATCCGCTCCAACACCTTCG-3'	202
	Reverse	5'-CGGCCTTAGCCTCTACCACC-3'	
aspC	Forward	5’- GCTGTTCCACGGCTGTTGC-3’	128
	Reverse	5’- CAAAGCCCTGATAGGCGAAGT-3’	
ppc	Forward	5’-TCGCCAAGTCCGATCTGTG-3’	114
	Reverse	5’- CCGCCTGAATATCTCGCTGTA-3’	
mqo	Forward	5'-AGCGTAATGACGATAACACCT-3'	232
	Reverse	5'-CCGTAAACCTTCGCCAGA-3'	
pykA	Forward	5'-ACGCCGTTCTGGATGGTA-3'	130
	Reverse	5'-ACGTTGATGCTCGGGATT-3'	

629

630

B: ***Klebsiella pneumoniae***

Gene	Primer	Primer sequence	Product size(bp)
16S rRNA	Forward	5'-CCTGGACAAAGACTGACGC-3'	104
	Reverse	5'-GGGCACAACCTCCAAATC-3'	
oadA	Forward	5'-CGTGGAGGTGGAAGGCAAAG-3'	91
	Reverse	5'-AGAGGCAGGAGCAGGAGCAG-3'	
oadB	Forward	5'-CACGGTGAGTAAGCGGGAGA-3'	110
	Reverse	5'-GGTTGCCGAAGCAGAACATC-3'	
oadC	Forward	5'-GGGCTTTGTGCTGGTGTTCC-3'	187
	Reverse	5'-AAGACGGCGATGGTGGTGA-3'	
mqo	Forward	5'-GCTCAGCACTACCACCACC-3'	166
	Reverse	5'-CAGTTTCCAGTCTTCTTTACGC-3'	
mqo2	Forward	5'-CGAAGGTCTACGGTCAGGC-3'	116
	Reverse	5'-CGAGAAGGTGGCGAATGGT-3'	
mdh	Forward	5'-AACTGTTCGGCGTTACCAC-3'	110
	Reverse	5'-GGAGTGACCACCAATGACC-3'	
pckA	Forward	5'-CCATCCGTCGAAGGTGATT-3'	208
	Reverse	5'-GTACTGGGTCGGGTGAAGC-3'	
pckA2	Forward	5'-ACTTCGTCGCCTTCAACCT-3'	82
	Reverse	5'-AACATCCCTTTCTTCATCTCG-3'	

C:***Vibrio parahaemolyticus***

Gene	Primer	Primer sequence	Product size(bp)
16S rRNA	Forward	5'-GCACAAGCGGTGGAGCAT-3'	202
	Reverse	5'-TCGCTGGCAAACAAGGAT-3'	
oadA	Forward	5'-CTTACTTATGCGTTGTTCC-3'	87
	Reverse	5'-CAATGTAGGTGCTGGTTC -3'	
oadB	Forward	5'-AGAAGAGGACATCAACCCAC-3'	155
	Reverse	5'-CGGAGCCAAGTACACCAG-3'	
mdh	Forward	5'-GATTGCGGTTGTTTGTCCTA-3'	83
	Reverse	5'-GAACTTCAGCAGCGATTGG-3'	
pck	Forward	5'-TACCGACTTCACTACCAGGTG-3'	93
	Reverse	5'-AGTCTTTCGCTTTGCTTTCC-3'	

634 **Table S10 related to M & M. Primers used for gene complementation**

Primer	Sequence(5'-3')
tdcE-S	GCTTATCATCGAT**AAGCTT**ATGAAGGTAGATATTGATAC
tdcE-AS	ATGCGTCCGGCGTAGA**GGATCC**TTAGAGCGCCTGGGTAAAGG
aceE-S	GCTTATCATCG**ATAAGC**TTATGTCAGAACGTTTCCCAAA
aceE-AS	CACGATGCGTCCGGCGTAGA**GGATCC**TTACGCCAGACGCGGGTTAA
lpdA-S	CGC**AAGCTT**ATGAGTACTGAAATCAAAAC
lpdA-AS	GCG**GGATCC**TTACTTCTTCTTCGCTTTCG
pykF-S	CGC**AAGCTT**ATGAAAAAGACCAAAATTGT
pykF-AS	GCG**GGATCC**TTAGTAGTGCCGCTCGGTAC
pflD-S	CGC**AAGCTT**ATGACGAATCGTATCTCTCG
pflD-AS	GCG**GGATCC**TTACAGCTGATGCGCTGTCC

635

636

637 **Table S11 Primers for PCK complementation**

Mutation site(s)		Primers
R65A	Forward	5’-accggtgcttcaccaaaagataagtatatcgtccgtgacgatacc-3’
	Reverse	5’-ttggtgaagcaccggtgaagatcccggtatcgacgg-3’
G209A	Forward	5’-tacggcgctgaaatgaagaaagggatgttctcgatgatgaactacctgc-3’
	Reverse	5’-tcatttcagcgccgtaccaggtgccgccaatcagct-3’
K212A	Forward	5’-gaaatggctgctgggatgttctcgatgatgaactacctgctgccgctg-3’
	Reverse	5’-catcccagcagccatttcgccgccgtaccaggtgcc-3’
H232A	Forward	5’-tctatggcgtgctccgccaacgttggtgagaaagg-3’
	Reverse	5’-cggagcacgccataga agcgatacctttcagcggcag-3’
S250A	Forward	5’-ggccttgcgggcaccg gtaaaaccacccttccacc-3’
	Reverse	5’-cggtgcccgcaaggcc gaagaacaccgcaacatcgc-3’
T256A	Forward	5’-aaaaccgcgctttcca ccgacccgaaacgtcgcctg-3’
	Reverse	5’-tggaaagcgcggtttt accggtgccggaaaggccga-3’
D268A/D269A	Forward	5’-attggcgctgctgaac acggctgggacgatgacggc-3’
	Reverse	5’-gttcagcagcgccaat caggcgacgtttcgggtcgg-3’
Y286A/K288A	Forward	5’-ggctgcgccgcagccact atcaagctgtcgaaagaagcggaacc -3’
	Reverse	5’-agtggctgcggcgcagcc gccttcgaagttaaacacgc-3’
E297A	Forward	5’-gaagcggcacctgaaa tctacaacgctatccgtcgt-3’
	Reverse	5’-tttcaggtgccgcttc tttcgacagcttgatagtttttgcgtagcagcc-3’
R333A	Forward	5’-aacaccgcggtttctt atccgatctatcacatcgat-3’

	Reverse	5’-aagaaaccgcggtgtt ctcggtttttgaaccatcat-3’
R449A	Forward	5’-ggcaaagctatctcg attaaagatacccgcgccattatcgacgccatcct-3’
	Reverse	5’-cgagatagctttgcc agtgccgttccagccagtgt-3’
I452A/T455A	Forward	5’-tcggcgaaagatgcgcgc gccattatcgacgccatcct-3’
	Reverse	5’-gcgcgcatctttcgccga gatagctttgccagtgccgt-3’

638
639
640
641